Highly Sensitive Electrochemical Determination of Isoproturon Based on Acetylene Black Nanoparticles Modified Glassy Carbon Electrode

Runqiang Liu[1], Xuli Hu[1], Yuanhang Cao[1], Haotian Pang[1], Wenlei Hou[1], Yansheng Shi[1], Haoming Li[1], Xinming Yin[2,*], Hongyuan Zhao[3,*]

[1] School of Resources and Environment, Henan Institute of Science and Technology, Xinxiang 453003, China
[2] College of Plant Protections, Henan Agricultural University, Zhengzhou 450002, China
[3] Henan Institute of Science and Technology, Xinxiang 453003, China
[*] E-mail: xmyin11@163.com; hongyuanzhao@126.com

The unreasonable use of isoproturon (ISO) had caused severe damage to human health and the ecological environment. Herein, an ultrasound-assisted strategy was proposed to construct a novel electrochemical sensor based on acetylene black (AB) nanoparticles for the sensitive determination of ISO. The morphological characterization of AB was investigated by scanning electron microscope (SEM), transmission electron microscopy (TEM), and X-ray diffraction (XRD). AB with pearl-chain-like carbon network exhibited outstanding electrical conductivity and prominent dispersion ability, which could significantly improve the electrochemical detection performance of ISO. The linear range of detecting ISO was 0.5-20 μM with the detection limit of 0.096 μM at the fabricated AB/GCE sensor. Moreover, the fabricated sensor demonstrated good stability, repeatability, and selectivity. The AB/GCE sensor presented acceptable recoveries of 98.21%-102.70% in measuring ISO in tomato and water samples. This work lays an essential foundation for using AB nanoparticles to develop high-performance ISO sensor.

1. INTRODUCTION

Isoproturon (ISO), a kind of phenylurea herbicide, is generally applied to prevent the growth of various worst weeds in the field of crops[1]. However, the ISO residues in waters, soils, and crops caused by unreasonable use would lead to a severe negative impact on the ecosystems and human health[2, 3]. Given this situation, a sensitive, efficient, and accurate detection method should be developed and used to determine ISO.

Recently, several traditional approaches are applied to the detection of ISO, such as high-performance liquid chromatography[4], capillary electrophoresis[5], and layer chromatography[6]. These technologies are of high importance to the determination of ISO owing to their excellent accuracy, while their large-scale applications are significantly limited by complex pretreatment procedures, time-consuming analysis, and high-cost equipment[2]. Compared with the above traditional methods, the electrochemical sensor has the advantages of inexpensive, simple fabrication, and high efficiency, presenting broad prospects in the field of pesticide detection[7-9]. Glassy carbon electrode (GCE), a common carbon-based electrode, is one of the most extensively employed in electroanalysis. It exhibits many majestic properties such as being polishable, chemically stable, compatible with more solutions, and impermeable[10].

According to existing reports, the modifications of the electrode play a crucial role in electrochemical performance[11]. Carbon-based material has emerged as an attractive candidate for the preparation of electrochemical sensors owing to its distinguishing property[12, 13]. Concerning the detection of ISO, some electrochemical sensors based on carbon-based materials have achieved satisfactory results[14-16]. Siham et al. prepared the electrochemical sensor using carbon nanotubes (CNTs) and copper oxide nanoparticles (CuO), and it was successfully applied in the detection of ISO[14]. Zhou et al. designed an electrochemical sensor of graphene oxide modified multi-walled carbon nanotubes hybridmaterial for the highly sensitive determination of ISO [15].

Acetylene black (AB), a kind of carbon nanomaterial with a porous structure, was produced from the thermal decomposition of calcium carbide gas in high-temp ericture[17]. Benefitting from the features of inexpensive, excellent conductivity[18], large specific surface area[19], strong adsorptive ability[20], and chemical stability[17], AB has been widely used in the field of batteries and electroanalytical sensors in recent years[21].

In this work, the AB/GCE was fabricated by a facile ultrasound-assisted method and successfully employed to determine ISO. The excellent electrical conductivity and strong adsorptive ability of AB remarkably enhanced the detection capability compared with the uncoated GCE sensor. The manufactured sensor exhibited a well linear range from 0.5 μM to 20 μM with a relatively low detection limit. In addition, this sensor showed great stability, reproducibility, and selectivity. The AB/GCE sensor possesses excellent practical feasibility for detecting ISO in water and vegetable samples, confirming that the AB/GCE sensor holds great promise for applications in pesticide detection fields.

2. EXPERIMENTAL

Acetylene black (AB) was provided by Timcal Co. Ltd. Isoproturon was supplied by Sinopharm Chemical Reagent Co. Ltd. Potassium chloride (KCl), sodium hydroxide (NaOH), phosphoric acid (H_3PO_4), Potassium ferricyanide ($K_3FeC_6N_6$), sodium phosphate dibasic (Na_2HPO_4), sodium dihydrogen phosphate (NaH_2PO_4), and N, N-dimethylformamide (DMF) were provided by Aladdin Co. Ltd. All reagents were used in the experiment with analytically pure($\geq$ 99%). The tomato sample was from the local Hualian Supermarket, and a river water sample was obtained from the East Lake in the Henan Institute of Science and Technology. Experiments were conducted with modified glassy carbon

electrodes, platinum wire, and saturated calomel as working electrodes, count electrodes, and reference electrodes, respectively.

Before the AB/GCE sensor was fabricated, the GCE was polished using aluminum powders of different particle sizes and then cleaned with the ultrasonic method. Afterward, 8 mg of AB was dispersed in 4 mL DMF and then ultrasonic-dispersed for 40 mins. In the end, the gained suspension (5 μL) was placed on the GCE surface.. After being dried with the infrared lamp, the AB/GCE-based electrochemical sensor was successfully prepared.

The morphological structure of AB nanomaterial was investigated in SEM (JEOL JSM-6360LV, Japan; Voltage: 5.0 kV) and TEM (FEI Talos F200S Super-X), and the physical phases were detected by XRD (Bruker DX-1000, Germany) analysis. The electrochemical redox behavior of ISO was analyzed in the solution of $K_3[Fe(CN)_6]$/KCl containing 0.2 mM KCl. The whole measurements of ISO were performed with a phosphate buffer solution (PBS 0.1M) as the electrolytic solution. Besides, the pH of PBS was adjusted by adding NaOH or H_3PO_4. The electrochemical measurements were completed on the CHI660E electrochemical workstation.

3. RESULTS AND DISCUSSION

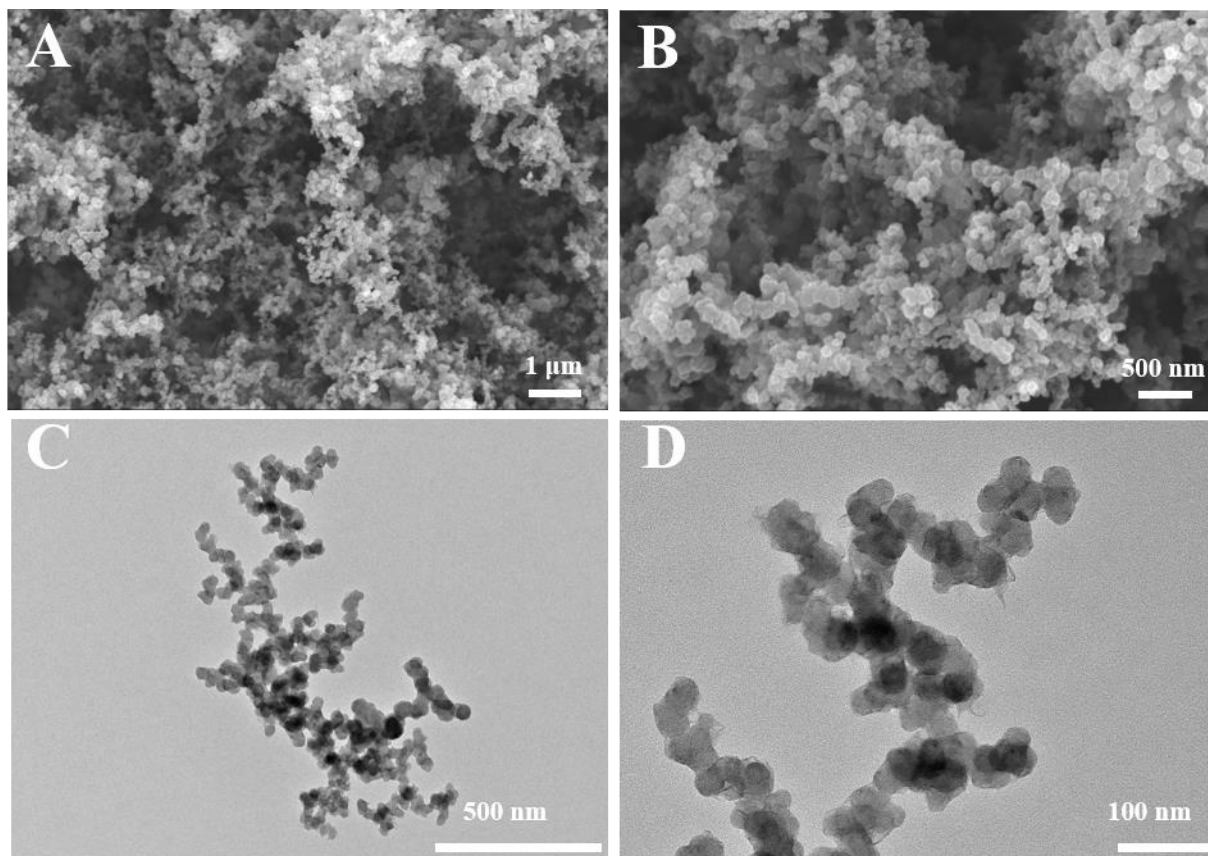## 3.1. Morphological structure of AB nanoparticles

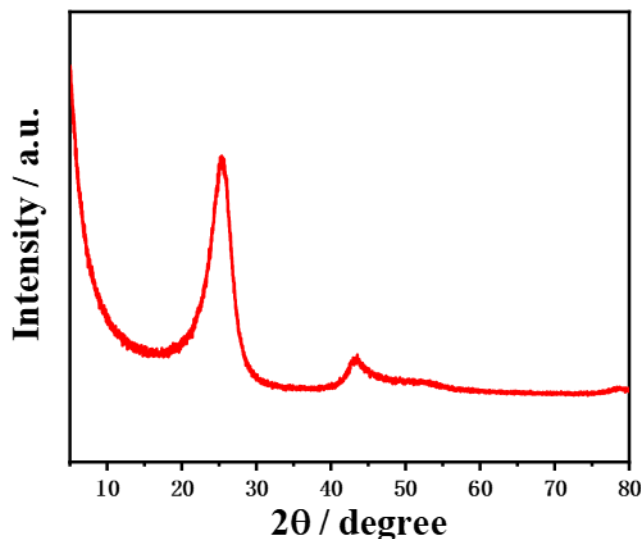**Figure 1.** (A and B) SEM and (C and D) TEM photographs of AB/GCE electrode

Figure 2. XRD pattern of AB nanoparticles.

As illustrated in **Fig. 1** A and B, AB nanoparticles presented homogenous particle distribution with the feature of high porous and loosened. In **Fig. 1** D and E, AB nanoparticles observed one-dimensional nanosphere-like microstructure, and the average diameter was ca. 30 nm. These particles connect with each other, resulting in a linked pearl-chain-like conductive network.

The XRD patterns peaks of AB can be observed in **Fig. 2**. AB exhibited two unambiguously diffraction peaks at about 25.5° and 42.5°, which could be indexed to the hexagonal graphite structure (JCPDS card No. 34-1832)[22, 23].

3.2. Electrochemical characterization

Fig. 3 A illustrated the CV curves of bare GCE and AB/GCE sensors. The redox peak of the bare electrode exhibited a smaller peak current (I_{pa} = 51.79 μA, I_{pc} = -55.07 μA). The electrochemical performance of the AB/GCE sensor improved considerably with bigger current values (I_{pa} = 71.45 μA, I_{pc}= -86.80 μA) after the bare electrode was treated with AB nanoparticles. This suggested that AB nanoparticles effectively enhanced the conductivity of the GCE sensor.

The results of EIS for two electrodes were provided in **Fig. 3** B, and the corresponding equivalent circuit also was inserted. The electrochemical property was intimately related to charging transfer resistance (R_{ct})[11]. The R_{ct} was estimated by the semicircular diameter[21]. Generally, the Nyquist diameter in the high-frequency area was positively correlated with the value of R_{ct}[15]. Compared to bare GCE, the AB/GCE possesses a smaller diameter (**Fig. 3** B), implying that its charge transfer resistance remarkably decreased. With outstanding electrical conductivity and a high surface-to-volume ratio[24] of AB nanoparticles, the constituted sensor presented superior electrocatalytic performance.
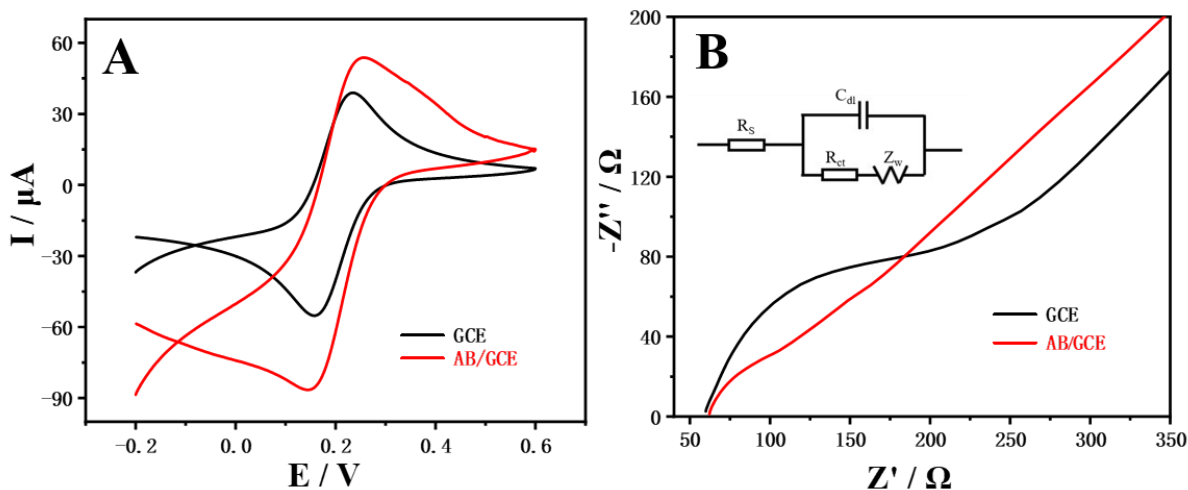
Figure 3. (A) CV curves of GCE and AB/GCE at 0.05 V s^{-1}. (B) Electrochemical impedance spectroscopy of GCE and AB/GCE (Redox probe: 5 mmol L^{-1} K$_3$[Fe(CN)$_6$] solution containing 0.2 mol L^{-1} KCl).

3.3 Electrochemical oxidation of ISO at the developed sensor

Fig. 4 exhibited the CV curves of two sensors at 10 µM ISO in PBS solution (0.1 M, pH 3.0). Only one oxidation peak is observed for each sensor, reflecting that the oxidation of ISO was an irreversible process. There was a weak oxidation peak in the bare GCE. After being modified with AB nanoparticles, the response current value (I$_{pa}$ = 9.216 µA) of ISO substantially increased. The excellent conductivity of AB nanoparticles was responsible for this phenomenon.

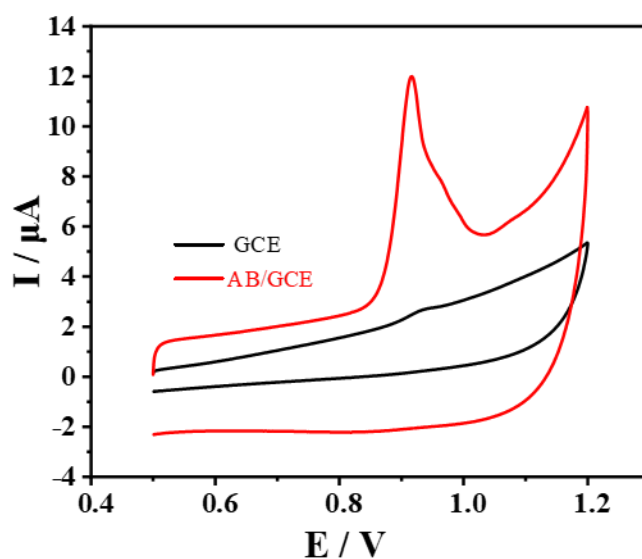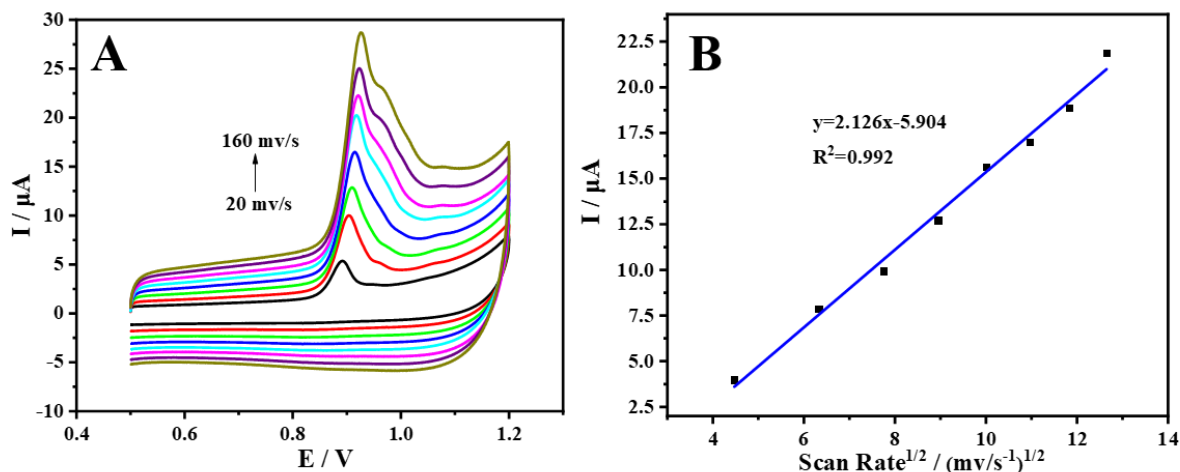**Figure 4.** Electrocatalytic oxidation of 10 µM ISO at unmodified GCE and AB/GCE sensors.

Figure 5. (A) CV curves of AB/GCE sensor in 10 µM ISO at a scan rate of 20-160 mV s^{-1}. (B) The linear graph corresponding scanning rate is 20, 40, 60, 80, 100, 120, 140, and 160 mV s^{-1}.

The impact of scan rates on the CV curve at the AB/GCE sensor was provided in **Fig. 5** A. The CV plots of the manufactured sensor were significantly affected by the scan rates. With the increase in the scanning rate, the CV oxidation peak currents increased. As demonstrated in **Fig. 5** B, the oxidation peak current was linearly associated with the square root of the scan rate with linear regression equations of $I(\mu A) = 2.126V^{1/2} - 5.904$ (R^2=0.992). This suggested a diffusion-controlled electrochemical response of ISO occurs at the AB/GCE sensor[16].

3.3 Experimental optimization

Fig. 6 depicted the effect of the pH value of the supporting electrolyte on the electrochemical behavior of ISO at the AB/GCE sensor.
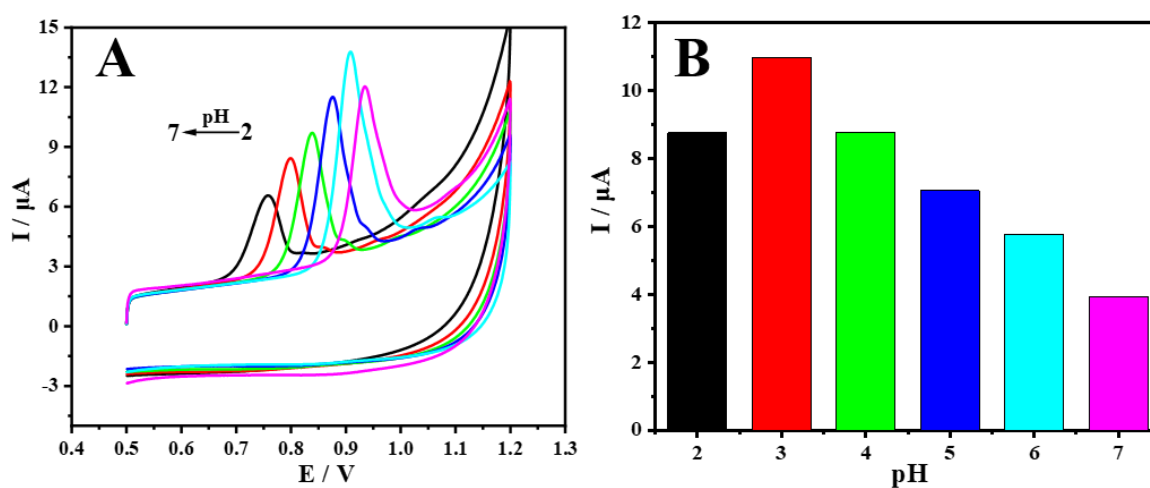

Figure 6. (A) CV response of 10 µM ISO at AB/GCE sensor in pH 2.0 - 7.0 reaction medium. (B) Effect of pH on oxidation peak current.
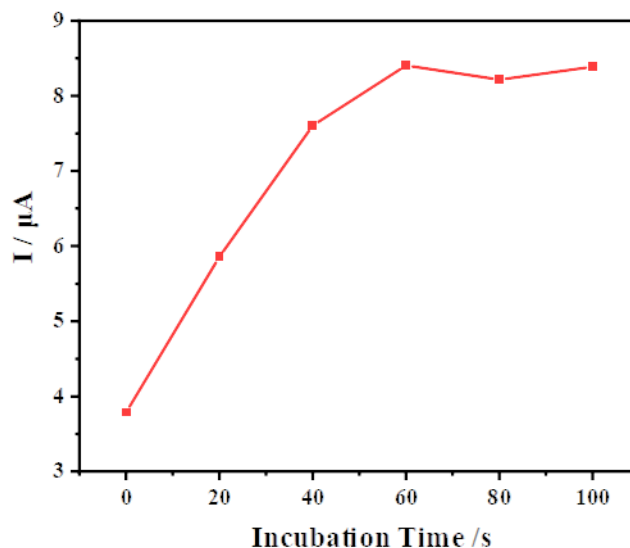
Figure 7. Effect of incubation times on the ISO determination performance.

The current first increased to a maximum and then decreased as pH increased. The oxidation peak current reached its maximum value at pH 3.0. Hence, the electrolyte with pH 3.0 was selected to obtain the highest sensitivity in the next work. Additionally, the peak potential of ISO shifted to higher values with increasing pH. This revealed the involvement of protons in the redox reaction process of the electrode[25].

The redox reaction on the electrode surface was always influenced by the enrichment time. As observed in **Fig. 7**, the oxidation peak current increased from 0 to 60 s. However, the current value did not increase anymore when the enrichment time exceeded 60 s. Considering the best test efficiency, the selected cumulative time was 60 s.

3.4 performance of the AB/GCE

The ISO with different concentrations at the AB/GCE sensor was measured at the optimal condition. As illustrated **Fig. 8** A, the peak current increased as the ISO concentration increased. Furthermore, the peak current has a linear relationship with ISO concentration in the range from 0.5 μM to 20 μM. In **Fig. 8** B, the corresponding regression equations was I (μA) = 0.5721 C + 0.1037 (R^2 = 0.992). The limit of detection was calculated as 0.096 μM (LOD = 3S/q, where "q" denoted the slope of the calibration plot and "S" represented the standard deviation attained from the blank measurements). Compared to the previously reported sensors (**Table 1**), the AB/GCE sensor exhibited a wider linear range and lower detection limit for ISO detection. AB nanoparticles with a pearl-chain structure formed an interconnected conductive network, which was beneficial to the electron transfer [20]. These results revealed that the established sensor had high sensitivity and well-accuracy.
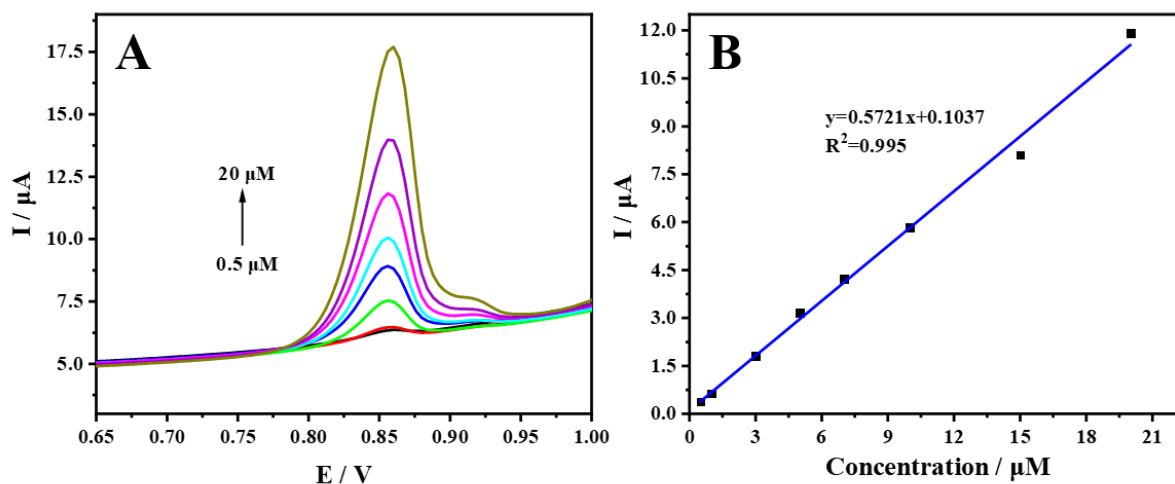
Figure 8. (A) DPV plots of ISO with several concentrations at the AB/GCE sensor. (B) Relationship of the peak current value and ISO concentration(0.5 - 20 μM).

3.5 Stability, repeatability, selectivity.

Stability, repeatability, and selectivity are key factors for the practical application of the developed sensor. Long-term stability was researched by measuring the same electrode stored in the refrigerator after a week. The peak current remained at about 85% of the previous current value, demonstrating the AB/GCE sensor displays strong stability.
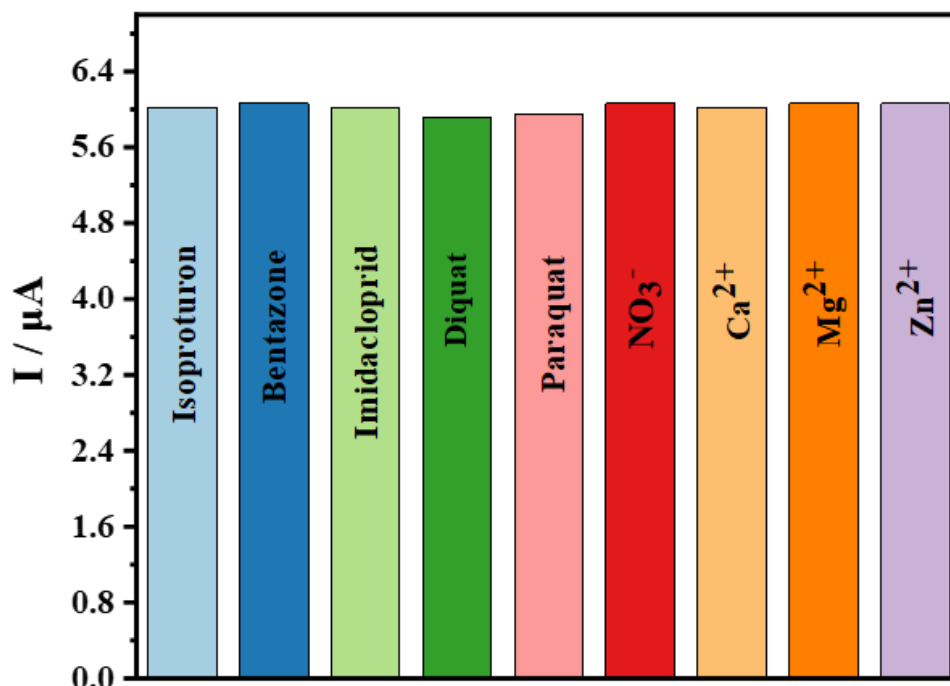

Figure 9. Selectivity of the AB/GCE sensor.

Table 1. Comparison of the synthesized sensor with various ISO sensors.

Electrode	Detectionmethod	LOD (μM)	Linear Range (μM)	Reference
Sodium montmorillonite/GCE	DPSV	4.12	0.206-61.8	[26]
Mesoporous silica film/GCE	SWV	—	10-100	[27]
Graphene/screen-printed electrode	SWSV	0.097	0.097-48.48	[2]
GO/MWCNTs-COOH/GCE	SWV	0.1	0.3-15	[15]
GCNTs@SP-Li/GCE	DPV	0.0946	0.7-30	[16]
MIP-GCE	SWV	0.0028	0–0.1	[28]
AB/GCE	DPV	0.0956	0.5-20	This work

Fig. 9 presented the effect of the electrochemical behavior of ISO at the AB/GCE sensor after the introduction of eight interferents (Bentazone, Imidacloprid, Diquat, Paraquat, NO_3^-, Ca^{2+}, Mg^{2+}, Zn^{2+}). It was demonstrated that the introduction of interfering substances has no significant effect on the electrochemical behavior of ISO. **Table 2** suggested that the the reproducibility and repeatability were measured using the same electrode and different electrodes, respectively. As a result, the RSD values of reproducibility and repeatability for six measurements were 1.90% and 0.90%, respectively. All these studies verified that the AB/GCE sensor possessed high stability, repeatability, and selectivity.

Table 2. Reproducibility and repeatability of the AB/GCE sensor.

Measurement	$I_1/\mu A$	$I_2/\mu A$	$I_3/\mu A$	$I_4/\mu A$	$I_5/\mu A$	$I_6/\mu A$	RSD (%)
The same sensors	5.93	5.90	6.20	6.01	6.02	6.12	1.90
Different sensors	6.02	6.02	6.01	6.16	6.08	6.05	0.90

3.6 Real sample analysis

Additionally, the river water and tomato samples were analyzed at the optimal condition using the standard addition method[29] to assess the validity of the AB/GCE sensor.

Table 3. Determination of ISO in real samples by using the DPV method.

Sample	Added (μM)	Found (μM)	Recovery (%)	RSD (%)
River water	4	3.96	99.05	2.11
	6	3.47	98.21	1.78
	8	7.97	99.67	1.31
Tomato	4	4.03	100.79	2.63
	6	6.07	101.23	0.59
	8	8.22	102.70	2.26

The actual water and vegetable juice samples were filtered by using a 0.22 μm filter membrane and then diluted for 100 multiples with PBS (pH 3.0). All samples were measured three times. The recovery and RSD values were calculated by averaging three measurements. As revealed in **Table 3**, three parallel samples exhibited recoveries ranging between 98.21 – 102.70%, and all RSD values were below 3%. These results confirmed that the AB/GCE sensor had high practical practicality.

4. CONCLUSION

In this paper, a simple and low-cost AB/GCE sensor was successfully fabricated based on AB nanoparticles for the determination of ISO. With the excellent conductive network and strong adsorptive ability of AB, the AB/GCE sensor displayed outstanding electrocatalytic activity for ISO detection. At optimal conditions, the prepared sensor possessed a board linear range of 0.5 - 20.0 μM, and the LOD value was 0.096 μM. Besides, the prepared sensor was adopted to detect water and tomato samples with satisfactory recoveries and low standard errors.

References

1. S. Zeng, X. Qin and L. Xia, *Biochem. Eng. J.,* 119 (2017) 92.
2. P. Noyrod, O. Chailapakul, W. Wonsawat and S. Chuanuwatanakul, *J. Electroanal. Chem.,* 719 (2014) 54.
3. J.C.G. Sousa, A.R. Ribeiro, M.O. Barbosa, M.F.R. Pereira and A.M.T. Silva, *J Hazard Mater.,* 344 (2018) 146.
4. S.R. Ruberu, W.M. Draper and S.K. Perera, *J. Agric. Food Chem.,* 48 (2000) 4109.
5. Y. Wang, L. Xiao and M. Cheng, *J Chromatogr A.,* 1218 (2011) 9115.
6. N. Badawi, S. Ronhede, S. Olsson, B.B. Kragelund, A.H. Johnsen, O.S. Jacobsen and J. Aamand, *Environ Pollut.,* 157 (2009) 2806.
7. T. Meng, L. Wang, H. Jia, T. Gong, Y. Feng, R. Li, H. Wang and Y. Zhang, *J. Colloid Interface Sci.,* 536 (2019) 424.
8. J. Yuan, L. Jiang, X. Tan, Y. Yue, H. Shi and S. Feng, *J. Electrochem. Soc.,* 167 (2020).
9. R. Liu, Y. Wang, B. Li, B. Liu, H. Ma, D. Li, L. Dong, F. Li, X. Chen and X. Yin, *Materials (Basel).,* 12 (2019).
10. S.I. Kaya, B. Demirkan, N.K. Bakirhan, E. Kuyuldar, S. Kurbanoglu, S.A. Ozkan and F. Sen, *J. Pharm. Biomed. Anal.,* 174 (2019) 206.
11. H. Zhao, Y. Chang, R. Liu, B. Li, F. Li, F. Zhang, M. Shi, L. Zhou and X. Li, *Food Chem.,* 343 (2021) 128484.
12. P.A. Sundari and P. Manisankar, *J. Braz. Chem. Soc.,* 22 (2011) 746.
13. R. Liu, Y. Wang, D. Li, L. Dong, B. Li, B. Liu, H. Ma, F. Li, X. Yin, X. Chen, *Int. J. Electrochem. Sci.,* 14 (2019) 9785.
14. S. Amra, T. Bataille, S.B. Bacha, M. Bourouina and D. Hauchard, *Electroanalysis.,* 32 (2020) 1346.
15. Y. Zhou, F. Cheng, Y. Hong, J. Huang, X. Zhang and X. Liao, *Food Anal. Methods.,* 13 (2020)

839.

16. D. Li, X. Hu, H. Zhao, K. Ding, F. Li, S. Han, H. Wang, L. Bai and R. Liu, *J. Porous Mater.,* (2022).
17. G. Jin, Z. Mingang, Y. Shijian, Y. Xiaoyan and W. Shiwei, *Ionics.,* 24 (2017) 2219.
18. Z. Deng, H. Li, Q. Tian, Y. Zhou, X. Yang, Y. Yu, B. Jiang, Y. Xu and T. Zhou, *Microchem. J.,* 157 (2020).
19. J. Song, J. Yang, J. Zeng, J. Tan and L. Zhang, *Microchimica Acta.* 171 (2010) 283.
20. M. Li, Y. Qi, Y. Ding, Q. Zhao, J. Fei and J. Zhou, *Sens. Actuators, B.,* 168 (2012) 329.
21. X. Zhang, J. Ma and K. Chen, *Nanomicro Lett.,* 7 (2015) 360.
22. H. Ibrahim, M. Ibrahim and Y. Temerk, *Talanta.,* 200 (2019) 324.
23. X. Liu, J.Z. Zhang, K.J. Huang and P. Hao, *Chem. Eng. J.,* 302 (2016) 437.
24. F.M. Morawski, J.P. Winiarski, C.E.M. de Campos, A.L. Parize and C.L. Jost, *Ecotoxicol Environ Saf.,* 206 (2020) 111181.
25. R. Wang, K. Wu and C. Wu, *Anal. Methods.,* 7 (2015) 8069.
26. P. Manisankar, G. Selvanathan and C. Vedhi, *Appl. Clay Sci.,* 29 (2005) 249.
27. T. Nasir, A. Gamero-Quijano, C. Despas, M. Dossot, G. Herzog and A. Walcarius, *Talanta.,* 220 (2020) 121347.
28. I. Sadriu, S. Bouden, J. Nicolle, F.I. Podvorica, V. Bertagna, C. Berho, L. Amalric and C. Vautrin-Ul, *Talanta.,* 207 (2020) 120222.
29. Xiaoyi Long, Chaorui Deng, Gansheng Xiao, Fuliang Cheng, Ying Zhou, Lei Zhao, Longfei Cai, Jinyin Chen, Juan Du, *Int. J. Electrochem. Sci.,* 15 (2020) 4964.